

Production of Charged Particles, K_S^0 , K^\pm , p and Λ in $Z \rightarrow b\bar{b}$ Events and in the Decay of b Hadrons

DELPHI Collaboration

Abstract

A sample of events enriched in $b\bar{b}$ quark pairs was selected in the data recorded by the DELPHI experiment at LEP during 1992 and 1993, by the presence of secondary decay vertices from short-lived particles. Using this sample, the average multiplicities of K_S^0 , K^\pm , $p(\bar{p})$, $\Lambda(\bar{\Lambda})$ and of charged particles in $b\bar{b}$ events have been measured, distinguishing the component from fragmentation and the component coming from the decay of b-hadrons. The measurement of the average charge multiplicity in $b\bar{b}$ events was used to compute the mean fractional beam energy carried by the primary b-hadron, and the difference in charged particle multiplicity between $b\bar{b}$ events and light quark ($u\bar{u}, d\bar{d}, s\bar{s}$) events.

(To be submitted to Physics Letters B)

P.Abreu²¹, W.Adam⁸, T.Adye³⁸, E.Agasi³¹, I.Ajinenko⁴³, R.Aleksan⁴⁰, G.D.Alekseev¹⁵, P.P.Allport²², S.Almehed²⁴, F.M.L.Almeida⁴⁸, S.J.Alvsvaag⁴, U.Amaldi⁸, S.Amato⁴⁸, A.Andreazza²⁸, M.L.Andrieux¹³, P.Antilogus²⁵, W-D.Apel¹⁶, Y.Arnoud⁴⁰, B.Åsman⁴⁵, J-E.Augustin¹⁹, A.Augustinus³¹, P.Baillon⁸, P.Bambade¹⁹, F.Barao²¹, R.Barate¹³, D.Y.Bardin¹⁵, G.J.Barker³⁵, A.Baroncelli⁴¹, O.Barring⁸, J.A.Barrio²⁶, W.Bartl⁵¹, M.J.Bates³⁸, M.Battaglia¹⁴, M.Baubillier²³, J.Baudot⁴⁰, K-H.Becks⁵³, M.Begalli³⁷, P.Beilliere⁷, Yu.Belokopytov⁸, P.Beltran¹⁰, A.C.Benvenuti⁵, M.Berggren⁴², D.Bertrand², F.Bianchi⁴⁶, M.Bigli⁴⁶, M.S.Bilenky¹⁵, P.Billoir²³, J.Bjarne²⁴, D.Bloch⁹, M.Blume⁵³, S.Blyth³⁵, V.Bocci³⁹, T.Bolognese⁴⁰, M.Bonesini²⁸, W.Bonivento²⁸, P.S.L.Booth²², G.Borisov⁴³, C.Bosio⁴¹, B.Bostjancic⁴⁴, S.Bosworth³⁵, O.Botner⁴⁹, B.Bouquet¹⁹, C.Bourdarios¹⁹, T.J.V.Bowcock²², M.Bozzo¹², P.Branchini⁴¹, K.D.Brand³⁶, R.A.Brenner¹⁴, C.Bricman², L.Brillault²³, R.C.A.Brown⁸, P.Bruckman¹⁷, J-M.Brunet⁷, L.Bugge³³, T.Buran³³, A.Buys⁸, M.Caccia²⁸, M.Calvi²⁸, A.J.Camacho Rozas⁴², T.Camporesi⁸, V.Canale³⁹, M.Canepa¹², K.Cankocak⁴⁵, F.Cao², F.Carena⁸, P.Carrilho⁴⁸, L.Carroll²², C.Caso¹², V.Cassio⁴⁶, M.V.Castillo Gimenez⁵⁰, A.Cattai⁸, F.R.Cavallo⁵, L.Cerrito³⁹, V.Chabaud⁸, A.Chan¹, M.Chapkin⁴³, Ph.Charpentier⁸, L.Chaussard²⁵, J.Chauveau²³, P.Checchia³⁶, G.A.Chelkov¹⁵, P.Chliapnikov⁴³, P.Chochula⁶, V.Chorowicz⁸, J.T.M.Chrin⁵⁰, V.Cindro⁴⁴, P.Collins⁸, J.L.Contreras¹⁹, R.Contri¹², E.Cortina⁵⁰, G.Cosme¹⁹, F.Cossutti⁴⁷, H.B.Crawley¹, D.Crennell³⁸, G.Crosetti¹², J.Cuevas Maestro³⁴, S.Czellar¹⁴, E.Dahl-Jensen²⁹, J.Dahm⁵³, B.Dalmagne¹⁹, M.Dam³³, G.Damgaard²⁹, A.Daum¹⁶, P.D.Dauncey³⁸, M.Davenport⁸, W.Da Silva²³, C.Defoix⁷, G.Della Ricca⁴⁷, P.Delpierre²⁷, N.Demaria³⁵, A.De Angelis⁸, H.De Boeck², W.De Boer¹⁶, S.De Brabandere², C.De Clercq², M.D.M.De Fez Laso⁵⁰, C.De La Vaissiere²³, B.De Lotto⁴⁷, A.De Min²⁸, L.De Paula⁴⁸, C.De Saint-Jean⁴⁰, H.Dijkstra⁸, L.Di Ciaccio⁹, F.Djama⁹, J.Dolbeau⁷, M.Donszelmann⁸, K.Doroba⁵², M.Dracos⁹, J.Drees⁵³, K.-A.Drees⁵³, M.Dris³², Y.Dufour⁷, F.Dupont¹³, D.Edsall¹, R.Ehret¹⁶, T.Ekelof⁴⁹, G.Ekspong⁴⁵, M.Elsing⁵³, J-P.Engel⁹, N.Ershaidat²³, M.Espirito Santo²¹, D.Fassouliotis³², M.Feindt⁸, A.Ferrer⁵⁰, T.A.Filippas³², A.Firestone¹, H.Foeth⁸, E.Fokitis³², F.Fontanelli¹², F.Formenti⁸, J-L.Fouisset²⁷, B.Franek³⁸, P.Frenkiel⁷, D.C.Fries¹⁶, A.G.Frodesen⁴, F.Fulda-Quenzer¹⁹, H.Furstenau⁸, J.Fuster⁸, D.Gamba⁴⁶, M.Gandelman¹⁸, C.Garcia⁵⁰, J.Garcia⁴², C.Gaspar⁸, U.Gasparini³⁶, Ph.Gavillet⁸, E.N.Gazis³², D.Gele⁹, J-P.Gerber⁹, D.Gillespie⁸, R.Gokieli⁵², B.Golob⁴⁴, J.J.Gomez Y Cadenas⁸, G.Gopal³⁸, L.Gorn¹, M.Gorski⁵², V.Gracco¹², F.Grard², E.Graziani⁴¹, G.Grosdidier¹⁹, P.Gunnarsson⁴⁵, J.Guy³⁸, U.Haedinger¹⁶, F.Hahn⁵³, M.Hahn¹⁶, S.Hahn⁵³, S.Haider³¹, Z.Hajduk¹⁷, A.Hakansson²⁴, A.Hallgren⁴⁹, K.Hamacher⁵³, W.Hao³¹, F.J.Harris³⁵, V.Hedberg²⁴, R.Henriques²¹, J.J.Hernandez⁵⁰, J.A.Hernando⁵⁰, P.Herquet², H.Herr⁸, T.L.Hessing⁸, E.Higon⁵⁰, H.J.Hilke⁸, T.S.Hill¹, S-O.Holmgren⁴⁵, P.J.Holt³⁵, D.Holthuisen⁵¹, P.F.Honore⁷, M.Houlden²², J.Hrubic⁵¹, K.Huet², K.Hultqvist⁴⁵, P.Ioannou³, J.N.Jackson²², R.Jacobsson⁴⁵, P.Jalocha¹⁷, R.Janik⁶, G.Jarlskog²⁴, P.Jarry⁴⁰, B.Jean-Marie¹⁹, E.K.Johansson⁴⁵, L.Jonsson²⁴, P.Juillot⁹, M.Kaiser¹⁶, G.Kalmus³⁸, F.Kapusta²³, M.Karlsson⁴⁵, E.Karvelas¹⁰, S.Katsanevas³², E.C.Katsoufis²², R.Keranen¹⁴, B.A.Khomenko¹⁵, N.N.Khovanski¹⁵, B.King²², N.J.Kjaer²⁹, H.Klein⁸, A.Klovning⁴, P.Kluit³¹, J.H.Koehne¹⁶, B.Koene³¹, P.Kokkinias¹⁰, M.Koratzinos⁸, K.Korczyk¹⁷, V.Kostioukhine⁴³, C.Kourkoumelis³, O.Kouznetsov¹², P.-H.Kramer⁵³, M.Krammer⁵¹, C.Kreuter¹⁶, J.Krolkowski⁵², I.Kronkvist²⁴, Z.Krumstiel¹⁵, W.Krupinski¹⁷, P.Kubinec⁶, W.Kucewicz¹⁷, K.Kulka⁴⁹, K.Kurvinen¹⁴, C.Lacasta⁵⁰, I.Laktineh²⁵, S.Lamblot²³, C.Lambropoulos¹⁰, J.W.Lamsa¹, L.Lanceri⁴⁷, D.W.Lane¹, P.Langefeld⁵³, V.Lapin⁴³, I.Last²², J-P.Laugier⁴⁰, R.Lauhakangas¹⁴, G.Leder⁵¹, F.Ledroit¹³, V.Lefebure², C.K.Legan¹, R.Leitner³⁰, Y.Lemoigne⁴⁰, J.Lemonne², G.Lenzen⁵³, V.Lepeltier¹⁹, T.Lesiak³⁶, D.Liko⁵¹, R.Lindner⁵³, A.Lipniacka¹⁹, I.Lippi³⁶, B.Loerstad²⁴, M.Lokajicek¹¹, J.G.Loken³⁵, A.Lopez-Fernandez⁸, M.A.Lopez Aguera⁴², D.Loukas¹⁰, J.J.Lozano⁵⁰, P.Lutz⁴⁰, L.Lyons³⁵, G.Maehlum¹⁶, J.Maillard⁷, A.Maio²¹, A.Maltezos¹⁰, V.Malychev¹⁵, F.Mandl⁵¹, J.Marco⁴², B.Marechal⁴⁸, M.Margoni³⁶, J-C.Marin⁸, C.Mariotti⁴¹, A.Markou¹⁰, T.Marou⁵³, C.Martinez-Rivero⁴², F.Martinez-Vidal⁵⁰, S.Marti i Garcia⁵⁰, F.Matorras⁴², C.Matteuzzi²⁸, G.Matthiae³⁹, M.Mazzucato³⁶, M.Mc Cubbin⁸, R.Mc Kay¹, R.Mc Nulty²², J.Medbo⁴⁹, C.Meroni²⁸, W.T.Meyer¹, M.Michelotto³⁶, E.Migliore⁴⁶, I.Mikulec⁵¹, L.Mirabito²⁵, W.A.Mitaroff⁵¹, U.Mjoernmark²⁴, T.Moa⁴⁵, R.Moeller²⁹, K.Moenig⁸, M.R.Monge¹², P.Morettini¹², H.Mueller¹⁶, W.J.Murray³⁸, B.Muryn¹⁷, G.Myatt³⁵, F.Naraghi¹³, F.L.Navarría⁵, S.Navas⁵⁰, P.Negri²⁸, S.Nemecek¹¹, W.Neumann⁵³, N.Neumeister⁵¹, R.Nicolaidou³, B.S.Nielsen²⁹, V.Nikolaenko²⁵, P.Niss⁴⁵, A.Nomerotski³⁶, A.Normand³⁵, W.Oberschulte-Beckmann¹⁶, V.Obraztsov⁴³, A.G.Olshevski¹⁵, R.Orava¹⁴, K.Osterberg¹⁴, A.Ouraou⁴⁰, P.Paganini¹⁹, M.Paganoni²⁸, P.Pages⁹, H.Palka¹⁷, Th.D.Papadopoulou³², L.Pape⁸, F.Parodi¹², A.Passerì⁴¹, M.Pegoraro³⁶, J.Pennanen¹⁴, L.Peralta²¹, V.Perevozchikov⁴³, H.Pernegger⁵¹, M.Pernicka⁵¹, A.Perrotta⁵, C.Petridou⁴⁷, A.Petrolini¹², H.T.Phillips³⁸, G.Piana¹², F.Pierre⁴⁰, M.Pimenta²¹, S.Plaszczynski¹⁹, O.Podobrin¹⁶, M.E.Pol¹⁸, G.Polok¹⁷, P.Poropat⁴⁷, V.Pozdniakov¹⁵, M.Prest⁴⁷, P.Privitera³⁹, A.Pullia²⁸, D.Radojicic³⁵, S.Ragazzi²⁸, H.Rahmani³², J.Rames¹¹, P.N.Ratoff²⁰, A.L.Read³³, M.Reale⁵³, P.Rebecchi¹⁹, N.G.Redaeli²⁸, M.Regler⁵¹, D.Reid⁸, P.B.Renton³⁵, L.K.Resvanis³, F.Richard¹⁹, J.Richardson²², J.Ridky¹¹, G.Rinaudo⁴⁶, I.Ripp⁴⁰, A.Romero⁴⁶, I.Roncagliolo¹², P.Ronchese³⁶, V.Ronjin⁴³, L.Roos¹³, E.I.Rosenberg¹, E.Rosso⁸, P.Roudeau¹⁹, T.Rovelli⁵, W.Ruckstuhl³¹, V.Ruhlmann-Kleider⁴⁰, A.Ruiz⁴², H.Saarikko¹⁴, Y.Sacquin⁴⁰, A.Sadovsky¹⁵, G.Sajot¹³, J.Salt⁵⁰, J.Sanchez²⁶, M.Sannino¹², H.Schneider¹⁶, M.A.E.Schyns⁵³, G.Sciolla⁴⁶, F.Scuri⁴⁷, Y.Sedykh¹⁵, A.M.Segar³⁵, A.Seitz¹⁶, R.Sekulin³⁸, R.C.Shellard³⁷, I.Siccama³¹, P.Siegrist⁴⁰, S.Simonetti⁴⁰, F.Simonetto³⁶, A.N.Sisakian¹⁵, B.Sitar⁶, T.B.Skaali³³, G.Smadjja²⁵, N.Smirnov⁴³, O.Smirnova¹⁵, G.R.Smith³⁸, R.Sosnowski⁵², D.Souza-Santos³⁷, T.Spaso²¹, E.Spiriti⁴¹, P.Sponholz⁵³, S.Squarcia¹², H.Staek⁵³, C.Stanescu⁴¹, S.Stapnes³³, I.Stavitski³⁶, G.Stavropoulos¹⁰, K.Stepaniak⁵², F.Stichelbaut⁸, A.Stocchi¹⁹, J.Strauss⁵¹, R.Strub⁹, B.Stugu⁴

M.Szczekowski⁵², M.Szeptycka⁵², T.Tabarelli²⁸, J.P.Tavernet²³, O.Tchikilev⁴³, G.E.Theodosiou¹⁰, A.Tilquin²⁷, J.Timmermans³¹, L.G.Tkatchev¹⁵, T.Todorov⁹, D.Z.Toet³¹, A.Tomaradze², B.Tome²¹, E.Torassa⁴⁶, L.Tortora⁴¹, G.Transtromer²⁴, D.Treille⁸, W.Trischuk⁸, G.Tristram⁷, A.Trombini¹⁹, C.Troncon²⁸, A.Tsirou⁸, M-L.Turluer⁴⁰, I.A.Tyapkin¹⁵, M.Tyndel³⁸, S.Tzamaras²², B.Ueberschaer⁵³, S.Ueberschaer⁵³, O.Ullaland⁸, V.Uvarov⁴³, G.Valenti⁵, E.Vallazza⁸, J.A.Valls Ferrer⁵⁰, G.W.Van Apeldoorn³¹, P.Van Dam³¹, W.K.Van Doninck², J.Van Eldik³¹, G.Vegni²⁸, L.Ventura³⁶, W.Venus³⁸, F.Verbeure², M.Verlato³⁶, L.S.Vertogradov¹⁵, D.Vilanova⁴⁰, P.Vincent²⁵, L.Vitale⁴⁷, E.Vlasov⁴³, A.S.Vodopyanov¹⁵, M.Voutilainen¹⁴, V.Vrba¹¹, H.Wahlen⁵³, C.Walck⁴⁵, F.Waldner⁴⁷, A.Wehr⁵³, M.Weierstall⁵³, P.Weilhammer⁸, A.M.Wetherell⁸, D.Wicke⁵³, J.H.Wickens², M.Wielers¹⁶, G.R.Wilkinson³⁵, W.S.C.Williams³⁵, M.Winter⁹, M.Witek⁸, G.Wormser¹⁹, K.Woschnagg⁴⁹, K.Yip³⁵, L.Yu³⁵, O.Yushchenko⁴³, F.Zach²⁵, A.Zaitsev⁴³, A.Zalewska¹⁷, P.Zalewski⁵², D.Zavrtanik⁴⁴, E.Zevgolatakos¹⁰, N.I.Zimin¹⁵, M.Zito⁴⁰, D.Zontar⁴⁴, R.Zuberi³⁵, G.C.Zucchelli⁴⁵, G.Zumerle³⁶

¹Ames Laboratory and Department of Physics, Iowa State University, Ames IA 50011, USA

²Physics Department, Univ. Instelling Antwerpen, Universiteitsplein 1, B-2610 Wilrijk, Belgium and IIHE, ULB-VUB, Pleinlaan 2, B-1050 Brussels, Belgium

and Faculté des Sciences, Univ. de l'Etat Mons, Av. Maistriau 19, B-7000 Mons, Belgium

³Physics Laboratory, University of Athens, Solonos Str. 104, GR-10680 Athens, Greece

⁴Department of Physics, University of Bergen, Allégaten 55, N-5007 Bergen, Norway

⁵Dipartimento di Fisica, Università di Bologna and INFN, Via Irnerio 46, I-40126 Bologna, Italy

⁶Comenius University, Faculty of Mathematics and Physics, Mlynska Dolina, SK-84215 Bratislava, Slovakia

⁷Collège de France, Lab. de Physique Corpusculaire, IN2P3-CNRS, F-75231 Paris Cedex 05, France

⁸CERN, CH-1211 Geneva 23, Switzerland

⁹Centre de Recherche Nucléaire, IN2P3 - CNRS/ULP - BP20, F-67037 Strasbourg Cedex, France

¹⁰Institute of Nuclear Physics, N.C.S.R. Demokritos, P.O. Box 60228, GR-15310 Athens, Greece

¹¹FZU, Inst. of Physics of the C.A.S. High Energy Physics Division, Na Slovance 2, 180 40, Praha 8, Czech Republic

¹²Dipartimento di Fisica, Università di Genova and INFN, Via Dodecaneso 33, I-16146 Genova, Italy

¹³Institut des Sciences Nucléaires, IN2P3-CNRS, Université de Grenoble 1, F-38026 Grenoble Cedex, France

¹⁴Research Institute for High Energy Physics, SEFT, P.O. Box 9, FIN-00014 Helsinki, Finland

¹⁵Joint Institute for Nuclear Research, Dubna, Head Post Office, P.O. Box 79, 101 000 Moscow, Russian Federation

¹⁶Institut für Experimentelle Kernphysik, Universität Karlsruhe, Postfach 6980, D-76128 Karlsruhe, Germany

¹⁷High Energy Physics Laboratory, Institute of Nuclear Physics, Ul. Kawiorów 26a, PL-30055 Krakow 30, Poland

¹⁸Centro Brasileiro de Pesquisas Físicas, rua Xavier Sigaud 150, BR-22290 Rio de Janeiro, Brazil

¹⁹Université de Paris-Sud, Lab. de l'Accélérateur Linéaire, IN2P3-CNRS, Bat 200, F-91405 Orsay Cedex, France

²⁰School of Physics and Materials, University of Lancaster, Lancaster LA1 4YB, UK

²¹LIP, IST, FCUL - Av. Elias Garcia, 14-1º, P-1000 Lisboa Codex, Portugal

²²Department of Physics, University of Liverpool, P.O. Box 147, Liverpool L69 3BX, UK

²³LPNHE, IN2P3-CNRS, Universités Paris VI et VII, Tour 33 (RdC), 4 place Jussieu, F-75252 Paris Cedex 05, France

²⁴Department of Physics, University of Lund, Sölvegatan 14, S-22363 Lund, Sweden

²⁵Université Claude Bernard de Lyon, IPNL, IN2P3-CNRS, F-69622 Villeurbanne Cedex, France

²⁶Universidad Complutense, Avda. Complutense s/n, E-28040 Madrid, Spain

²⁷Univ. d'Aix - Marseille II - CPP, IN2P3-CNRS, F-13288 Marseille Cedex 09, France

²⁸Dipartimento di Fisica, Università di Milano and INFN, Via Celoria 16, I-20133 Milan, Italy

²⁹Niels Bohr Institute, Blegdamsvej 17, DK-2100 Copenhagen 0, Denmark

³⁰NC, Nuclear Centre of MFF, Charles University, Areal MFF, V Holesovickach 2, 180 00, Praha 8, Czech Republic

³¹NIKHEF-H, Postbus 41882, NL-1009 DB Amsterdam, The Netherlands

³²National Technical University, Physics Department, Zografou Campus, GR-15773 Athens, Greece

³³Physics Department, University of Oslo, Blindern, N-1000 Oslo 3, Norway

³⁴Dpto. Fisica, Univ. Oviedo, C/P. Pérez Casas, S/N-33006 Oviedo, Spain

³⁵Department of Physics, University of Oxford, Keble Road, Oxford OX1 3RH, UK

³⁶Dipartimento di Fisica, Università di Padova and INFN, Via Marzolo 8, I-35131 Padua, Italy

³⁷Depto. de Fisica, Pontificia Univ. Católica, C.P. 38071 RJ-22453 Rio de Janeiro, Brazil

³⁸Rutherford Appleton Laboratory, Chilton, Didcot OX11 0QX, UK

³⁹Dipartimento di Fisica, Università di Roma II and INFN, Tor Vergata, I-00173 Rome, Italy

⁴⁰Centre d'Etude de Saclay, DSM/DAPNIA, F-91191 Gif-sur-Yvette Cedex, France

⁴¹Istituto Superiore di Sanità, Ist. Naz. di Fisica Nucl. (INFN), Viale Regina Elena 299, I-00161 Rome, Italy

⁴²C.E.A.F.M., C.S.I.C. - Univ. Cantabria, Avda. los Castros, S/N-39006 Santander, Spain, (CICYT-AEN93-0832)

⁴³Inst. for High Energy Physics, Serpukov P.O. Box 35, Protvino, (Moscow Region), Russian Federation

⁴⁴J. Stefan Institute and Department of Physics, University of Ljubljana, Jamova 39, SI-61000 Ljubljana, Slovenia

⁴⁵Fysikum, Stockholm University, Box 6730, S-113 85 Stockholm, Sweden

⁴⁶Dipartimento di Fisica Sperimentale, Università di Torino and INFN, Via P. Giuria 1, I-10125 Turin, Italy

⁴⁷Dipartimento di Fisica, Università di Trieste and INFN, Via A. Valerio 2, I-34127 Trieste, Italy and Istituto di Fisica, Università di Udine, I-33100 Udine, Italy

⁴⁸Univ. Federal do Rio de Janeiro, C.P. 68528 Cidade Univ., Ilha do Fundão BR-21945-970 Rio de Janeiro, Brazil

⁴⁹Department of Radiation Sciences, University of Uppsala, P.O. Box 535, S-751 21 Uppsala, Sweden

⁵⁰IFIC, Valencia-CSIC, and D.F.A.M.N., U. de Valencia, Avda. Dr. Moliner 50, E-46100 Burjassot (Valencia), Spain

⁵¹Institut für Hochenergiephysik, Österr. Akad. d. Wissensch., Nikolsdorfergasse 18, A-1050 Vienna, Austria

⁵²Inst. Nuclear Studies and University of Warsaw, Ul. Hoza 69, PL-00681 Warsaw, Poland

⁵³Fachbereich Physik, University of Wuppertal, Postfach 100 127, D-42097 Wuppertal 1, Germany

1 Introduction

The comparison of $Z \rightarrow b\bar{b} \rightarrow \text{hadrons}$ with $u\bar{u}, d\bar{d}, s\bar{s} \rightarrow \text{hadrons}$ is relevant for the understanding of multiparticle production mechanisms and for testing hadronization models. While measurements of the average charged particle multiplicity in $b\bar{b}$ events at the Z peak exist [1–3], this analysis presents the first results on the average multiplicities of identified particles such as K_S^0 , K^\pm , p and Λ , and their momentum spectra, in $b\bar{b}$ and in the decay of b-hadrons¹. The mixture of b-hadrons at LEP differs from that at the $\Upsilon(4S)$ because of the presence of B_s^0 and b-baryons.

The DELPHI Ring Imaging Cherenkov Detector (RICH) is used for the identification of charged particles.

A new method is proposed for distinguishing leading from non-leading hadrons, based on the rapidity with respect to the thrust axis. This variable displays a good separation, and it is rather independent of the assumptions on the fragmentation and decay models (see Figure 1 a, b and c for charged particles, K^0 and Λ respectively). This allows the separation of the b-hadron decay from fragmentation products, and to measure the relevant branching fractions of b-hadrons.

The difference in charge multiplicity between events initiated by b and uds quarks, δ_{bl} , is also measured and the results compared with different QCD based models, which predict both the absolute value for δ_{bl} and its behaviour as a function of centre-of-mass energy. In addition, the mean value of the fractional beam energy carried by the primary b-hadron is inferred from the mean charged particle multiplicity measurement in $b\bar{b}$ events, by means of the JETSET 7.3 Monte Carlo model [4].

2 Experimental Method

The sample of events used in this analysis was accumulated during 1992 and 1993 with the DELPHI detector at the LEP e^+e^- collider, operating at centre-of-mass energies on or around the Z peak. The sample corresponds to a total of 1 272 895 hadronic decays of the Z.

A description of DELPHI can be found in reference [5]. Features of the apparatus relevant for this analysis are outlined in reference [6]. The analysis presented here relies on the information provided by the central tracking detectors: the Micro Vertex Detector (VD), the Inner Detector (ID), the Time Projection Chamber (TPC), the Barrel Ring Imaging Cherenkov Detector (RICH) and the Outer Detector (OD).

- The VD consisted of 3 cylindrical layers of silicon micro-strip detectors, at radii 6.3, 9.0 and 11.0 cm. They measure $R\phi$ (transverse to the beam) coordinates over a length along the beam of 24 cm. The polar angle coverage of the VD extends from 42° to 138° .
- The ID is a cylindrical drift chamber (inner radius 12 cm and outer radius 22 cm) covering polar angles between 29° and 151° .
- The TPC, the main tracking device of DELPHI, is a cylinder of 30 cm inner radius, 122 cm outer radius and has a length of 2.7 m. Each end-cap is divided into 6 sector plates, each with 192 sense wires used for the particle identification. The energy loss per unit length (dE/dx) is measured by these wires as the 80% truncated mean of the amplitudes of the wire signals. A dE/dx measurement is considered to be significant if at least 30 wires contribute to it. About 25% of the charged particles

¹Unless otherwise stated, antiparticles are implicitly included.

with momentum, p , above 1 GeV/ c have no dE/dx information either because of too few hits or because of overlapping tracks.

- The OD consists of 5 layers of drift cells at radii between 192 and 208 cm, covering polar angles between 43° and 137° .
- The Barrel RICH [7] covers the polar angle between 40° and 140° . It identifies the charged particles by measuring the angle of emission of Cherenkov light, and thus the velocity. The mass of the charged particle is then extracted by combining the velocity information with the momentum measurement. In order to cover a large momentum range (1 to 20 GeV/ c), the DELPHI Barrel RICH uses two different Cherenkov radiators, one liquid (C_6F_{14}) and one gaseous (C_5F_{12}).

The central tracking system of DELPHI covers the region between 25° and 155° in polar angle, θ . The average momentum resolution for the charged particles in hadronic final states is in the range $\Delta p/p \simeq 0.001p$ to $0.01p$ (p in GeV/ c), depending on which detectors are included in the track fit.

Charged particles were used in the analysis if they had:

- (i) momentum larger than 0.1 GeV/ c ;
- (ii) measured track length in the TPC greater than 25 cm;
- (iii) θ between 25° and 155° ;
- (iv) relative error on the measured momentum smaller than 100%.

Hadronic events were then selected by requiring that:

(α) the total energy of the charged particles in the event exceeded 12% of the centre of mass energy;

(β) there were at least 5 charged particles with momenta above 0.2 GeV/ c .

In the calculation of the energies, all charged particles have been assumed to have the pion mass.

Events due to beam-gas scattering and to $\gamma\gamma$ interactions have been estimated to be less than 0.1% of the sample; background from $\tau^+\tau^-$ events was calculated to be less than 0.2%.

The influence of the detector on the analysis was studied with the simulation program DELSIM [8]. Events were generated with the

- (a) JETSET 7.3 Parton Shower (PS) Monte Carlo program [4] with parameters tuned by DELPHI (in particular, the Peterson fragmentation function [9] was used for heavy quarks). The particles were followed through the detailed geometry of DELPHI giving simulated digitizations in each detector. These data were processed with the same reconstruction and analysis programs as the real data.

Simulations based on:

- (b) HERWIG 5.7, with cluster fragmentation [10];
- (c) JETSET 7.4 PS, with string fragmentation and Bowler parametrization of the fragmentation function;
- (d) JETSET 7.3 PS with Lund symmetric fragmentation function;
- (e) ARIADNE[11], with dipole fragmentation

were also used to estimate the systematic errors. The average energies of b-hadrons in these simulation programs, normalized to the beam energy, were respectively 0.70 for (a), 0.67 for (b), 0.69 for (c), 0.74 for (d) and 0.70 for (e).

2.1 b-Tagging

Event samples of different flavour content were obtained by using a lifetime tag algorithm, originally developed by the ALEPH Collaboration [12] and adapted for DELPHI data [13]. It is constructed from the lifetime signed impact parameter [14] of charged particles, d_i , in the r, ϕ plane. Defining the impact parameter significance of each track by $S = d_i/\sigma_i$, where σ_i is the measured error on d_i , and selecting only those tracks with negative values of S , which principally emanate from hadrons coming directly from the primary vertex, allows a resolution function for S to be constructed directly from the data. The resolution function can then be applied to define a probability function $P(S_0)$, that gives the probability of a track originating from the primary vertex to have an absolute significance value of S_0 or greater. In the present analysis, an impact parameter tag is formulated by combining the probabilities of those tracks with positive S within a given hemisphere, as determined by the plane perpendicular to the thrust axis, to give an event hemisphere probability of P_h :

$$P_h \equiv \Pi \sum_{j=0}^{N-1} \frac{(-\ln \Pi)^j}{j!},$$

where

$$\Pi \equiv \prod_{i=1}^N P(S_i).$$

By construction, P_h gives the probability for the N tracks in a given hemisphere to be consistent with all coming from the primary vertex.

In this paper, unless otherwise stated, hemispheres opposite to those for which P_h is less than 0.001 were selected. This gives a b purity of 91.8% for the selected sample of hemispheres. The contamination from $c\bar{c}$ events was estimated to be 5.0%, while the remaining 3.2% is due to light quark-antiquark pairs. The selection efficiency is about 17% for events with thrust axis contained in the VD acceptance.

2.2 Selection of V^0 Candidates

K_S^0 and Λ candidates were detected by their decay in flight into $\pi^+\pi^-$ and $p\pi^-$ respectively.

Candidate secondary decays, V^0 , in the selected sample of hadronic events were found by considering all pairs of oppositely charged particles. The vertex defined by each such pair was determined such that the χ^2 of the hypothesis of a common vertex was minimized. The tracks were then refitted to the common vertex.

The V^0 decay vertex candidates were required to satisfy the following:

- the probability of the χ^2 fit to the vertex was larger than 0.01;
- in the $R\phi$ plane, the angle between the vector sum of the charged particle momenta and the line joining the primary to the secondary vertex was less than $(10 + 20/p_t)$ mrad, where p_t is the transverse momentum of the V^0 candidate relative to the beam axis, in GeV/ c ;
- the radial separation of the primary and secondary vertex in the $R\phi$ plane was greater than four standard deviations;
- when the reconstructed decay point of the V^0 was beyond the VD radius, there were no signals in the VD consistent with association to the decay tracks;
- the transverse momentum of each particle of the V^0 with respect to the line of flight was larger than 0.02 GeV/ c .

The $\pi^+\pi^-$ and $p\pi^-$ ($\bar{p}\pi^+$) invariant masses (attributing to the track of larger momentum the proton (antiproton) mass) for the candidates passing the cuts listed above were calculated. The average detection efficiency from this procedure is about 36% for $K_S^0 \rightarrow \pi^+\pi^-$ and about 28% for $\Lambda \rightarrow p\pi^-$ in multihadronic events.

The $\pi\pi$ and $p\pi$ invariant mass spectra after the cuts listed above are shown in Figure 2a and 2b respectively. From Figure 2a, it is clearly visible that our simulation, based on JETSET, overestimates the K_S^0 production; this happens especially in the low momentum region [15]. By parameterizing the signal with a double Gaussian (which accounts for the variation of the width as a function of the momentum) one has $13334 \pm 171 K_S^0$ and $3444 \pm 164 \Lambda$ in the selected sample. The weighted average width is about $5.4 \text{ MeV}/c^2$ for K_S^0 and $2.4 \text{ MeV}/c^2$ for Λ .

In the analysis presented in this paper, the numbers of reconstructed K_S^0 and Λ in a given kinematical region were estimated by fitting the invariant mass spectra of the candidates with a double Gaussian, and by parametrizing the background with a polynomial. The K_S^0 signal was also estimated by fitting a polynomial form to the invariant mass distribution having excluded the mass window between 0.48 and 0.52 GeV/c^2 and then subtracting that estimated background from the total number of candidates in the signal region. To complete the estimation of the systematic errors the order of the polynomial used to parametrize the background was varied and different mass windows were used in the fits.

Reconstruction efficiencies were calculated by generating hadronic Z decays with the JETSET 7.3 PS model [4], passing them through the DELSIM Monte Carlo simulation program [8] in the same way as the data and then comparing the simulated with the generated distributions. These efficiencies also included the corrections for the relevant branching fractions.

2.3 K^\pm and p

K^\pm and p were selected by using the information provided by both the Barrel RICH and the energy loss in TPC.

In the Barrel RICH, for each mass hypothesis ($e/\mu/\pi/K/p$), the signal detected is compared to the sum of the expected signal for the given momentum, plus a background extracted from the data. From this a likelihood probability is computed [7,16]. Quality cuts and cuts on the likelihood probabilities are set. For example, to select a kaon its probability is required to be above 30%, and the number of photoelectrons after background subtraction should be less than 20. For the energy loss by ionization in TPC, the measured value of dE/dX has to be within 3 standard deviations of the value expected for a kaon and 3 standard deviations outside the value expected for pions.

The information coming from dE/dX and from the RICH are combined. The full detector simulation is used to estimate the efficiency and the rejection factor. Selected track samples (pions from K_S^0 decays, protons from Λ and K^\pm from D^0) are used to check simulation predictions.

The efficiency for the identification of a K^\pm , averaged over the momentum spectrum above 0.7 GeV/c , was estimated from simulation to be 64% with a contamination of 34% in the sample selected for this analysis. The average efficiency for the identification of a proton was estimated to be about 65% with a contamination of 56%. The conservative systematic uncertainties used for this analysis were $\pm 15\%$ on the tagging efficiencies and $\pm 30\%$ on the contaminations.

3 Analysis and Results

3.1 Charged particles

3.1.1 Average multiplicity

In order to extract the true multiplicity distribution, F_n , from that measured, F_m , an acceptance matrix, A_{mn} was constructed using the JETSET Monte Carlo generator [4] with full detector simulation to account for the event and track selection efficiencies and for the additional spurious tracks arising from hadron interactions in the detector material and from photon conversions:

$$A_{mn} = \frac{M_{mn}^{MC}}{N_n^{MC}}.$$

Here, N_n^{MC} is the number of simulated events generated with multiplicity n , including contributions from charged particles resulting from K_S^0 and Λ decays, while M_{mn}^{MC} gives the number of events generated with multiplicity n but observed with multiplicity m . Thus, by construction, the elements of the acceptance matrix A_{mn} denote the probability of an event with original multiplicity n to be observed as an event registering m charged particles, and are at first order independent of the shape of the multiplicity distribution of the simulation at generator level. The original multiplicity distribution, F_n , is then unfolded from that observed, F_m , by a maximum likelihood method using the function:

$$F_m = \sum_n A_{mn} F_n ,$$

where F_n is represented by the Negative Binomial distribution [17] whose free parameters give the true mean multiplicity, $\langle n \rangle$, and the dispersion, D . The overall normalization factor, which gives the total number of events corrected for detector acceptance, was also allowed to vary in the fit. This procedure corrects also for the cuts related to the selection of multihadronic events. The method was extensively tested on fully simulated events and in all cases the Negative Binomial distribution was able to reproduce the mean of the true multiplicity to within 0.2%.

The method was first applied to all hadronic events from which a value for the mean hemisphere multiplicity of 10.569 ± 0.002 was measured, in good agreement with that obtained from a multiplicity analysis appearing in a previous publication [18].

Cuts on the hemisphere probability, P_h , were then applied in order to select samples of events enriched in (1) b and (2) uds contents. A third sample (3) containing very approximately the nominal quark flavour ratios was also selected in order to constrain the charm contribution to the hemisphere multiplicity measurements. A c -enriched sample of events could not however be obtained owing to the lack of sensitivity of the lifetime tag algorithm to the charm contribution.

The mean hemisphere multiplicity, $\langle n_h \rangle$, of these three samples was then unfolded, computing separately for each sample the acceptance matrix. The results together with the hemisphere probability cuts applied and the corresponding fractions of q -type quarks f_q , as determined from the simulation, are shown in Table 1.

In each of the three samples, the average multiplicity $\langle n_h \rangle$ is a linear combination of the unknowns $\langle n_h \rangle_b$, $\langle n_h \rangle_{uds}$ and $\langle n_h \rangle_c$. One can thus formulate a set of three simultaneous equations to compute these unknowns. Factors $C_q^{(i)}$ multiplying the coefficients f_q were introduced to account for possible biases introduced by the application of the hemisphere probability cuts; these factors were computed by means of the

Sample	Hemisphere Probability	f_b	f_{uds}	f_c	$\langle n_h \rangle$
(1)	$P_h < 0.0001$	0.951	0.018	0.031	11.557 ± 0.038
(2)	$0.8 < P_h < 1.0$	0.049	0.822	0.129	10.331 ± 0.014
(3)	$0.01 < P_h < 0.8$	0.163	0.645	0.192	10.571 ± 0.006

Table 1: Measured mean hemisphere multiplicities, $\langle n_h \rangle$, in three event samples of different flavour content, f_q , selected by applying cuts on the hemisphere probability, P_h .

simulation².

$$\langle n_h \rangle^{(1)} = f_b^{(1)} C_b^{(1)} \langle n_h \rangle_b + f_{uds}^{(1)} C_{uds}^{(1)} \langle n_h \rangle_{uds} + f_c^{(1)} C_c^{(1)} \langle n_h \rangle_c ,$$

$$\langle n_h \rangle^{(2)} = f_b^{(2)} C_b^{(2)} \langle n_h \rangle_b + f_{uds}^{(2)} C_{uds}^{(2)} \langle n_h \rangle_{uds} + f_c^{(2)} C_c^{(2)} \langle n_h \rangle_c ,$$

$$\langle n_h \rangle^{(3)} = f_b^{(3)} C_b^{(3)} \langle n_h \rangle_b + f_{uds}^{(3)} C_{uds}^{(3)} \langle n_h \rangle_{uds} + f_c^{(3)} C_c^{(3)} \langle n_h \rangle_c .$$

Solving the above equations gave the following mean charged particle multiplicities for a single hemisphere:

$$\begin{aligned} \langle n_h \rangle_b &= 11.66 \pm 0.04 , \\ \langle n_h \rangle_c &= 10.92 \pm 0.16 , \\ \langle n_h \rangle_{uds} &= 10.10 \pm 0.04 . \end{aligned}$$

The relatively large uncertainty of the measured mean multiplicity for charm stems from the inability of the P_h variable to extract a c-enriched sample of events. From the hemisphere measurements appearing in Table 1, the difference in average total charged multiplicity between $b\bar{b}$ events, $\langle n \rangle_{b\bar{b}}$, and light quark events (uds), $\langle n \rangle_{\Pi}$, is then computed to be:

$$\delta_{bl} = \langle n \rangle_{b\bar{b}} - \langle n \rangle_{\Pi} = 2(\langle n_h \rangle_b - \langle n_h \rangle_{uds}) = 3.12 \pm 0.09 .$$

Systematic uncertainties affect the shape of the impact parameter distribution of tracks used in the construction of the hemisphere probability, P_h , and consequently affect the determination of the flavour content as a function of P_h . Such uncertainties were investigated by means of the simulation. The main physics sources of these uncertainties arise from the assumed lifetime of b-hadrons ($\tau_b = 1.52 \pm 0.04$ ps) [19], the D^+ , D^0 lifetimes and production rates [20], the Z branching ratios into heavy quark pairs [21] and the heavy quark fragmentation functions [22]. Uncertainties in the determination of the resolution function and in the bias coefficients, C_q^i , were also investigated. In the latter case, the uncertainty was estimated by solving the simultaneous equations assuming no correlation between hemispheres, i.e. with $C_q^i = 1$. The larger systematic error on δ_{bl} , in comparison to $\langle n_h \rangle_b$, is a consequence of the large overlap in the P_h distribution between c and uds events, making the extraction of the light quark multiplicity less precise than that of the b.

In addition, uncertainties due to the detector acceptance and the track and event selections were investigated by varying the selection criteria. A further systematic error, due to photon conversions in the material of the detector, was estimated by varying

²The $C_q^{(i)}$ should be all equal to one if there was no correlation between hemispheres; despite the fact that the cuts were applied to the jet *opposite* to that being analyzed, small correlations were nevertheless observed, which affect the determination of $\langle n_h \rangle_b$ at the level of 1%.

their number in the simulation by $\pm 10\%$. These uncertainties affect mainly the absolute multiplicity values rather than the multiplicity difference, δ_{bl} , and are estimated to be about ± 0.22 for $\langle n_h \rangle_b$. The analysis was repeated with different cuts applied to the hemisphere probability, P_h , and the results obtained did not differ significantly. A b enriched sample of events was also selected by demanding in the opposite jet the presence of a muon with large momentum ($p > 7 \text{ GeV}/c$) and large transverse momentum with respect to the jet axis ($p_T > 1.1 \text{ GeV}/c$). The b purity of the sample obtained was approximately 83%, as estimated from the simulation, and the resulting analysis of the hemisphere opposite to that containing the lepton yielded measurements of $\langle n_h \rangle_b = 11.39 \pm 0.10$ and $\delta_{bl} = 2.68 \pm 0.16$, which is consistent with the result from the lifetime tag analysis and is largely subject to different systematic uncertainties.

The final mean values of the *event* multiplicity in b events, $\langle n \rangle_{b\bar{b}}$, taken as twice that of $\langle n_h \rangle_b$, and the multiplicity difference between $b\bar{b}$ and light quark-antiquark events, are thus:

$$\langle n \rangle_{b\bar{b}} = 23.32 \pm 0.08 \pm 0.50 , \quad (1)$$

$$\delta_{bl} = 3.12 \pm 0.09 \pm 0.67 . \quad (2)$$

These values include the products of K_S^0 and Λ decays.

3.1.2 Comparison with QCD Models

According to QCD in the modified leading logarithmic approximation (MLLA), the effective cut off for the emission of gluons from quarks is directly proportional to the mass of the quark and takes the form $\Theta_0 = m_q/E_q$ [23,24]. For the heavy b quarks, there is thus a resulting suppression of gluons in the forward direction around the b quark. When further invoking the hypothesis of local parton hadron duality (LPHD) [25], the predicted restriction of gluon emission in the forward direction is then expected to manifest itself in a suppression of the multiplicity of light hadrons accompanying the decay products of the b-hadrons when compared with that arising from events initiated by the light uds quarks at the same centre-of-mass energy [24]. The extent of this corresponding loss in particle production has been the subject of recent theoretical study [26–28]. The most remarkable aspect to have arisen from these investigations is the realization that the expected depletion in the so called ‘companion’ (nonleading) multiplicity, which refers to the *light* quark multiplicity which accompanies the decay products of the primary hadrons, is *independent* of the centre-of-mass energy W - a striking prediction given the rise of average multiplicity with W . Quantitatively, Petrov and Kisselev [27] have evaluated a rigorous upper bound for the multiplicity difference, δ_{bl} , of $\delta_{bl} < 3.7 - 4.1$, with the exact value depending on the b quark mass. A less rigorous derivation of the absolute value gives $\delta_{bl} = 3.68$ at $W = 91 \text{ GeV}$ for $m_b = 4.8 \text{ GeV}/c^2$ [27].

However, in an alternative (‘modified naive’) model [27,29], the companion multiplicity in an event is governed by the effective energy available to the fragmentation system following the production of the primary hadrons with energy fraction, $x_E = 2 \cdot E_{hadron}/W$.

The JETSET 7.3 Parton Shower model [4], when used to express the dependence on W of the energy fraction carried by leading hadrons in $b\bar{b}$ and in light quark-antiquark events, predicts a δ_{bl} of 4.2 ± 0.4 at 29 GeV and 1.8 ± 0.3 at 91 GeV, with a further error of order ± 0.5 due to the uncertainty associated with the estimate of the light quark event multiplicity variation with centre-of-mass energy.

The available results on δ_{bl} from different centre-of-mass energies [30] are displayed in Figure 3, together with the theoretical predictions. The data, although statistically limited at the lower centre-of-mass energies, remains compatible with the MLLA prediction

of an energy independent multiplicity difference, δ_{bl} . This is exemplified by a straight line fit of the form $\delta_{bl} = gW + d$, which yields values of $g = -0.024 \pm 0.016 \text{ GeV}^{-1}$ and $d = 5.3 \pm 1.2$ with a χ^2/DF of 1.0/3. Assuming zero gradient, $g = 0$, gives a value for the constant, d , of 3.5 ± 0.4 with a χ^2/DF of 3.5/4. The average of δ_{bl} from LEP and SLC experiments is also seen to lie within the QCD upper bound of $\delta_{bl} < 4.1$ and is in reasonable agreement with the less precise prediction for the absolute value of $\delta_{bl} = 3.68$ assuming $m_b = 4.8 \text{ GeV}/c^2$.

3.1.3 b Fragmentation

A measurement of $\langle n \rangle_{b\bar{b}}$ can further be used to provide information on the fragmentation of b quarks into b-hadrons, in terms of the mean scaled energy variable, $\langle x_E \rangle = 2 E_{hadron}/W$, where E_{hadron} is the energy of the b-hadron and W is the centre-of-mass energy [26,29,31]. The method relies on distinguishing between “leading” and “non-leading” multiplicity contribution to $\langle n \rangle_{b\bar{b}}$. The “leading” event multiplicity is the number of charged particles from the decay of the two primary hadrons, $n_{b\bar{b}}^B$, while the “non-leading” multiplicity is that due to the remainder of the fragmentation system, $n_{b\bar{b}}^{nl}$. While the former depends only on the type of b-hadrons produced, the latter is governed by the energy available to the fragmenting system, E^{nl} , whose mean value is determined from the heavy quark fragmentation function by the simple relationship $\langle x_E \rangle_B = 1 - \langle E \rangle^{nl}/W$. The relationship between $\langle n \rangle_{b\bar{b}}^{nl}$ and $\langle E \rangle^{nl}$, or equivalently $\langle x_E \rangle_B$, was determined using JETSET 7.3 PS incorporating parameters tuned to fit LEP data. The fragmentation function used was that of Peterson [9], whose free parameter, ϵ_b , was varied across a wide range of values.

The mean multiplicity of b-hadrons has been measured at the $\Upsilon(4S)$ [32] and recently at the Z resonance [2] (see also next section). The values at the two centre-of-mass energies agree within the errors, although the composition of b flavoured hadrons is different. Assuming, as in previous studies [1], $\langle n \rangle_{b\bar{b}}^B = 11.0 \pm 0.2$ at the Z peak, then the non-leading multiplicity is found to be:

$$\langle n \rangle_{b\bar{b}}^{nl} = \langle n \rangle_{b\bar{b}} - \langle n \rangle_{b\bar{b}}^B = 12.32 \pm 0.08 \pm 0.54 .$$

This results in a mean scaled energy for b-hadrons (B) of:

$$\langle x_E \rangle_B = 0.688 \pm 0.004 \pm 0.028 . \quad (3)$$

Systematic errors arising from uncertainties in the value of the QCD scale parameter and in the knowledge of the precise form of the heavy quark fragmentation function, which affect the relationship between $\langle n \rangle_b^{nl}$ and $\langle x_E \rangle_B$, are small by comparison. The above result corresponds to a value of $\epsilon_b = 0.008 \begin{smallmatrix} - \\ + \end{smallmatrix} \begin{smallmatrix} 0.004 \\ 0.007 \end{smallmatrix}$ as used in the JETSET Monte Carlo model.

3.1.4 Multiplicity Distribution and Momentum Spectrum

This analysis was based on the sample of data taken during 1993, corresponding to 30113 hemispheres from 631849 hadronic events.

The distribution in the variable $\xi_p = -\ln(p/p_{beam})$ for charged particles in $b\bar{b}$ events is plotted in Figure 4a and tabulated in Table 2. In the figure and the table, the distributions are compared with all events [33].

We have computed the multiplicity with a method similar to that described in [18]. The probability of having n charged particles in a b hemisphere, $P_b(n)$, was computed as

$$P_b(n) = P_b^{MC}(n) + P_{enriched}^{DATA}(n) - P_{enriched}^{MC}(n)$$

ξ_p -interval	$(1/2\sigma)d\sigma/d\xi_p, b$	$(1/2\sigma)d\sigma/d\xi_p, \text{all ev}$
0.0 - 0.2	—	0.009 ± 0.002
0.2 - 0.4	0.005 ± 0.001	0.034 ± 0.004
0.4 - 0.6	0.030 ± 0.003	0.105 ± 0.007
0.6 - 0.8	0.099 ± 0.006	0.198 ± 0.009
0.8 - 1.0	0.211 ± 0.009	0.324 ± 0.011
1.0 - 1.2	0.366 ± 0.012	0.510 ± 0.014
1.2 - 1.4	0.583 ± 0.016	0.715 ± 0.016
1.4 - 1.6	0.926 ± 0.021	0.991 ± 0.020
1.6 - 1.8	1.313 ± 0.025	1.262 ± 0.022
1.8 - 2.0	1.742 ± 0.030	1.544 ± 0.024
2.0 - 2.2	2.153 ± 0.033	1.834 ± 0.026
2.2 - 2.4	2.646 ± 0.036	2.112 ± 0.028
2.4 - 2.6	2.954 ± 0.038	2.375 ± 0.030
2.6 - 2.8	3.199 ± 0.039	2.628 ± 0.031
2.8 - 3.0	3.393 ± 0.040	2.824 ± 0.032
3.0 - 3.2	3.600 ± 0.041	3.002 ± 0.032
3.2 - 3.4	3.678 ± 0.041	3.085 ± 0.033
3.4 - 3.6	3.684 ± 0.041	3.199 ± 0.034
3.6 - 3.8	3.656 ± 0.040	3.186 ± 0.033
3.8 - 4.0	3.565 ± 0.039	3.175 ± 0.033
4.0 - 4.2	3.321 ± 0.038	3.116 ± 0.034
4.2 - 4.4	3.119 ± 0.037	3.014 ± 0.034
4.4 - 4.6	2.712 ± 0.034	2.736 ± 0.032
4.6 - 4.8	2.396 ± 0.031	2.444 ± 0.031
4.8 - 5.0	1.930 ± 0.027	2.201 ± 0.031
5.0 - 5.2	1.556 ± 0.023	1.844 ± 0.029
5.2 - 5.4	1.187 ± 0.019	1.324 ± 0.023
5.4 - 5.6	0.864 ± 0.015	0.945 ± 0.020
5.6 - 5.8	0.622 ± 0.012	0.609 ± 0.017
5.8 - 6.0	0.417 ± 0.011	0.394 ± 0.019

Table 2: *Differential cross section for charged particles production in b hemispheres and in untagged hemispheres as a function of ξ_p .*

$$P_{enriched}^{DATA}(n) = \frac{\sum_m A_{mn} a(m)}{\mathcal{N}},$$

where $P_b^{MC}(n)$ is the probability (in the simulation at generator level) of having n charged particles in a $b\bar{b}$ event, $P_{enriched}^{MC}(n)$ is the same probability in the b-enriched simulated sample, A_{mn} is computed by simulation and gives the probability that an event with m observed charged particles comes from events with n charged particles, $a(m)$ is the true number of events with m charged particles, and \mathcal{N} is a normalization factor such that $P_{enriched}^{DATA}$ is normalized to unity. The absolute value of the difference between $P_b^{MC}(n)$ and $P_{enriched}^{MC}(n)$ was taken as an estimate of the systematic error.

The distribution of multiplicity in b hemispheres is plotted in Figure 4b and tabulated in Table 3. The figure also compares the multiplicity distribution in the b hemispheres to that of the non-tagged sample. From the b multiplicity a value of $\langle n \rangle_{b\bar{b}} = 23.02 \pm 0.06(stat)$ was obtained which is consistent with the determination above (see Equation 1).

3.1.5 Average Decay Multiplicity of b-Hadrons

The rapidity distribution $r(|y|)$ (with respect to the thrust axis of the event) of charged particles opposite to a b-tagged hemisphere (Figure 5a) was corrected bin by bin using

n	$P_b(n)$	$P_q(n)$
1	—	0.124 ± 0.020
2	0.147 ± 0.024	0.466 ± 0.065
3	0.501 ± 0.036	1.21 ± 0.17
4	1.57 ± 0.12	2.67 ± 0.10
5	2.79 ± 0.21	4.56 ± 0.17
6	5.46 ± 0.38	7.04 ± 0.26
7	6.66 ± 0.48	8.58 ± 0.31
8	9.04 ± 0.57	9.97 ± 0.36
9	9.45 ± 0.52	10.20 ± 0.36
10	10.11 ± 0.44	9.87 ± 0.35
11	9.64 ± 0.29	8.85 ± 0.32
12	8.79 ± 0.18	7.83 ± 0.28
13	7.66 ± 0.22	6.44 ± 0.23
14	6.32 ± 0.27	5.19 ± 0.19
15	5.16 ± 0.31	4.14 ± 0.15
16	4.50 ± 0.32	3.22 ± 0.12
17	3.17 ± 0.29	2.490 ± 0.094
18	2.54 ± 0.28	1.980 ± 0.077
19	1.93 ± 0.25	1.400 ± 0.056
20	1.33 ± 0.21	1.04 ± 0.14
21	1.03 ± 0.17	0.76 ± 0.10
22	0.82 ± 0.15	0.591 ± 0.081
23	0.54 ± 0.10	0.426 ± 0.059
24	0.384 ± 0.085	0.285 ± 0.040
25	0.258 ± 0.064	0.212 ± 0.031
26	0.191 ± 0.054	0.128 ± 0.019
27	0.126 ± 0.044	0.076 ± 0.014
28	0.081 ± 0.029	0.041 ± 0.007
29	0.062 ± 0.028	0.042 ± 0.021
30	—	0.015 ± 0.005

Table 3: *Probability distribution for charged particle multiplicity in b hemispheres and in all events (%)*.

the simulation for detector effects, for correlations between hemispheres and for the contamination from non- $b\bar{b}$ events, giving the rapidity distributions for $b\bar{b}$ events. This was then fitted to the expression

$$r(|y|) = N((1 - \alpha)f_f(|y|) + \alpha f_d(|y|)) \quad (4)$$

where f_f and f_d are the distributions expected from fragmentation and decays of b -hadrons respectively, α is the fraction of particles arising from the decay of the b -hadron, and N is a normalization factor. Taking f_f and f_d from JETSET PS model with Peterson fragmentation gives $\alpha = 0.501 \pm 0.003$, with a χ^2 of 20.7 on 17 degrees of freedom. The result of the fit from this model was used for the measurement, because it was shown to reproduce the inclusive distributions reasonably well. By taking the distributions f_f and f_d from the different models mentioned in Section 2, different results on the fraction α of particles coming from the b -hadron decay were obtained; the RMS spread of these measurements was used as an estimate of the systematic error from this source. A second source of systematic error includes the effect of an additional uncertainty of $\pm 10\%$ (uncorrelated) on the efficiency for each rapidity bin, to account for possible rapidity-dependent effects. By folding these results with equation (1), the average number of charged particles from the decay of a b -hadron is:

$$n(B \rightarrow \text{Charged } X) = 5.84 \pm 0.04(\text{stat}) \pm 0.38(\text{syst}). \quad (5)$$

From the mixture of b-hadrons produced at LEP energies, OPAL has recently measured an average charged decay multiplicity of $5.51 \pm 0.05 \pm 0.51$ [2].

3.2 K_S^0 and Λ

The total yields of K_S^0 and Λ in $b\bar{b}$ events were calculated by integrating the efficiency corrected momentum distributions measured in the hemisphere opposite to the b-tagged hemisphere as described in [15,34].

The above integrals were corrected for the contamination from non- $b\bar{b}$ events assuming that the production rate of K_S^0 and Λ is that measured in inclusive production in hadronic Z decays [15,34]. The resulting production rates are:

$$\langle K_S^0 \rangle_{b\bar{b}} = 1.08 \pm 0.03(stat) \pm 0.05(syst) \quad (6)$$

$$\langle \Lambda \rangle_{b\bar{b}} = 0.338 \pm 0.021(stat) \pm 0.042(syst) \quad (7)$$

where the systematic error accounts for the background subtraction, the efficiency corrections, extrapolation to the invisible momentum region and the non- $b\bar{b}$ contamination.

To estimate the fraction of K_S^0 and Λ from the decays of b-hadrons, the measured rapidity distributions with respect to the thrust axis opposite a b-tagged hemisphere were compared with the distributions predicted by JETSET 7.3 PS model with Peterson fragmentation, as in Section 3.1.5.

Since the reconstruction efficiencies for both K_S^0 and Λ depend on the momentum, rather than the rapidity, the predictions from the simulation were weighted by means of visibility weights computed as a function of momentum.

In the following the measured rapidity distributions were fitted to the expression (4) by minimizing the quantity

$$\bar{R} \cdot V^{-1} \cdot R \quad (8)$$

where

R_i is a vector with elements $R_i = m(|y_i|) - r(|y_i|)$

$m(|y_i|)$ is the measurement for the rapidity bin i

$r(|y_i|)$ is the prediction for the rapidity bin i

V is the covariance matrix that accounts for statistical correlations between the rapidity bins. These correlations arise because each rapidity bin contains events from across the momentum range and the efficiencies are a strong function of momentum.

The fits resulted in the following average multiplicities:

$$n(B \rightarrow K_S^0 X) = 0.290 \pm 0.011 \quad (9)$$

$$n(B \rightarrow \Lambda X) = 0.059 \pm 0.007. \quad (10)$$

Figures 5b and 5c show the comparison of the uncorrected measured rapidity distributions with respect to the thrust axis with the results of the fits.

In the above, no account is taken in the fits to the rapidity distribution of the differences between measured and predicted momentum spectra. Since our simulation severely overestimates the K_S^0 production rate, especially in the low momentum region where the fragmentation production is dominant, a reweighting procedure was applied. The predictions of the momentum spectra of the fragmentation and B-decay components were scaled to fit the measured momentum distributions. The resulting momentum spectra were used to reweight the simulated events on an event by event basis from which new predictions of the rapidity distributions were found. The covariance matrix V in the

expression (8) was modified in order to include the scaling errors due to the uncertainty on our measured momentum spectra. By repeating the minimization of (8) the following results were found: $n(B \rightarrow K_S^0 X) = 0.274 \pm 0.015$, and $n(B \rightarrow \Lambda X) = 0.063 \pm 0.011$.

In order to check possible systematic effects due to performing the analysis with respect to the thrust axis another vector was formed to estimate the direction of the b-hadron. Neutral and charged reconstructed particles with rapidity greater than 1.5 with respect to the thrust axis were used to define a b-axis using the vector sum of their momenta. Such a vector is a good approximation of the b-hadron direction as shown in [35]. The rapidity distributions of K_S^0 and Λ defined with respect to this b-axis were compared as before with the predictions from the simulation. Using JETSET 7.3 model with Peterson fragmentation the results of the fit were: $n(B \rightarrow K_S^0 X) = 0.300 \pm 0.010$, and $n(B \rightarrow \Lambda X) = 0.048 \pm 0.008$. By using the reweighted distributions the following average multiplicities were obtained: $n(B \rightarrow K_S^0 X) = 0.279 \pm 0.015$, and $n(B \rightarrow \Lambda X) = 0.057 \pm 0.012$.

All the measurements were used to calculate the uncertainties due to the momentum spectra and choice of the reconstructed B direction, with the results (9) and (10) used as the central values. Finally we obtain:

$$n(B \rightarrow K_S^0 X) = 0.290 \pm 0.011 \pm 0.027 \quad (11)$$

$$n(B \rightarrow \Lambda X) = 0.059 \pm 0.007 \pm 0.009. \quad (12)$$

The first error includes the statistical error, the systematic error coming from the fits to the invariant mass spectra and from the rapidity distribution fit. The second error gives the RMS deviation of the four measurements combined with an estimation of the variation in the final results (9% for the K_S^0 and 13% for the Λ) if the other models listed in Section 2 were used to predict the rapidity distributions.

The branching fraction of nonstrange B mesons into Λ plus anything has been measured at the $\Upsilon(4S)$ to be $(4.0 \pm 0.5)\%$ [20]. If one neglects the difference between the B_s and the nonstrange mesons, and assumes that the fraction of b-baryons produced in the hadronization of a b quark is $(8 \pm 2)\%$ (this fraction is well determined by the probability of exciting a diquark-antidiquark pair from the vacuum [36]), then the branching fraction of any b-baryon (Λ_b) into Λ plus anything is determined as

$$Br(\Lambda_b \rightarrow \Lambda X) = 0.28_{-0.12}^{+0.17}.$$

In this result, the branching fraction was constrained to be larger than zero and smaller than one.

3.3 K^\pm and p

In this study, a sample of events collected during 1992, and in which both the gaseous and the liquid radiators in the Barrel RICH were operating, was used. This sample corresponds to 118 498 selected hadronic events. The b tagging algorithm selected 4 651 of them. Both hemispheres were studied in this case, since there is no reason for the b-tagging algorithm to bias the K^\pm and p content.

The rapidity distribution of the K^\pm and protons in b-tagged events was studied.

For each interval of the absolute value of rapidity (with respect to the thrust axis), the number of K^\pm and protons was computed for real data and for events coming from the full detector simulation. The simulation was then used to correct the data for detector effects, for a possible bias coming from the selection of b hemispheres, for correlations

between hemispheres and for the contamination from non- $b\bar{b}$ events, giving the rapidity distributions for $b\bar{b}$ events.

The rapidity distribution for K^\pm is shown in Figure 5d.

By summing the contents of the bins of the rapidity distribution, for $|y| < 3.8$ and extrapolating to the unobserved region by means of JETSET 7.4, we obtain the average number of K^\pm and p per hadronic ($b\bar{b}$) event:

$$\langle K^\pm \rangle_{b\bar{b}} = 2.74 \pm 0.10(stat) \pm 0.49(syst) \quad (13)$$

$$\langle p \rangle_{b\bar{b}} = 1.13 \pm 0.05(stat) \pm 0.26(syst). \quad (14)$$

The systematic error assumes in a conservative way an uncertainty of $\pm 15\%$ on the detection efficiency, and of $\pm 30\%$ on the contamination.

Using JETSET 7.3 PS + Peterson fragmentation to model f_f and f_d , the fractions of K^\pm and (anti)protons from the decay of b-hadrons were measured to be 0.639 ± 0.025 ($\chi^2/NDF = 13.1/17$) and 0.249 ± 0.029 ($\chi^2/NDF = 38.5/17$). By using the same procedure as in Section 3.1.5, the average number of K^\pm and (anti)protons from the decay of a b-hadron is:

$$n(B \rightarrow K^\pm X) = 0.88 \pm 0.05(stat) \pm 0.18(syst) \quad (15)$$

$$n(B \rightarrow pX) = 0.141 \pm 0.018(stat) \pm 0.056(syst). \quad (16)$$

The systematic error accounts for an uncertainty of $\pm 15\%$ on the efficiency as a function of rapidity, and for a correlated uncertainty of $\pm 30\%$ on the background.

4 Summary and Discussion

The average multiplicities of K_S^0 , K^\pm , (anti)proton, $\Lambda(\bar{\Lambda})$ and charged particles in $b\bar{b}$ events from the decay of the Z have been measured to be

$$\langle K_S^0 \rangle_{b\bar{b}} = 1.08 \pm 0.03(stat) \pm 0.05(syst)$$

$$\langle K^\pm \rangle_{b\bar{b}} = 2.74 \pm 0.10(stat) \pm 0.49(syst)$$

$$\langle p \rangle_{b\bar{b}} = 1.13 \pm 0.05(stat) \pm 0.26(syst)$$

$$\langle \Lambda \rangle_{b\bar{b}} = 0.338 \pm 0.021(stat) \pm 0.042(syst)$$

$$\langle n \rangle_{b\bar{b}} = 23.32 \pm 0.08(stat) \pm 0.50(syst).$$

The average number of K_S^0 per $b\bar{b}$ event is about 1.5 standard deviations higher than the average yield in hadronic events (0.981 ± 0.030) as measured by DELPHI [15].

The difference in multiplicity between Z^0 decays giving b and uds quarks has been measured to be:

$$\delta_{bl} = 3.12 \pm 0.09(stat) \pm 0.67(syst).$$

This result lies within the QCD upper bound prediction of $\delta_{bl} < 4.1$ and is in reasonable agreement with the less precise prediction for the absolute value of $\delta_{bl} = 3.68$ for $m_b = 4.8 \text{ GeV}/c^2$. It is not however consistent with the naive model approach which assumes that the non-leading multiplicity in $b\bar{b}$ events is the same as that in light quark events of energy equivalent to that of the fragmenting system in $b\bar{b}$ events.

The mean charged hadron multiplicity was used to extract a value for the mean scaled energy taken by the primordial b-hadron of:

$$\langle x_E \rangle_B = 0.688 \pm 0.004(stat) \pm 0.028(syst),$$

in good agreement with measurements from inclusive lepton and other types of analyses [22].

The DELPHI results on multiplicities in $b\bar{b}$ events are compared with the predictions from JETSET 7.4 PS and HERWIG 5.7, and with results at the Z peak for untagged $q\bar{q}$ events [37], in Table 4. JETSET PS accounts for the observed results both in tagged $b\bar{b}$ events and untagged events, except that it predicts a too large K_S^0 fraction in both samples.

	LEP+SLC, $q\bar{q}$	J74, $q\bar{q}$	HERWIG, $q\bar{q}$	DELPHI, $b\bar{b}$	J74, $b\bar{b}$	HERWIG, $b\bar{b}$
$\langle K_S^0 \rangle$	1.020 ± 0.018	1.10	1.04	1.08 ± 0.06	1.24	1.40
$\langle K^\pm \rangle$	2.35 ± 0.10	2.29	2.27	2.74 ± 0.50	2.66	3.16
$\langle p \rangle$	0.98 ± 0.09	1.16	0.99	1.13 ± 0.27	0.94	0.63
$\langle \Lambda \rangle$	0.367 ± 0.010	0.38	0.46	0.338 ± 0.047	0.29	0.27
$\langle n \rangle$	20.92 ± 0.19	21.0	20.3	23.32 ± 0.51	23.3	26.6

Table 4: Average multiplicities measured by experiments at the Z peak for multihadronic events and by DELPHI for $b\bar{b}$ events, compared with the predictions from JETSET 7.4 PS and HERWIG 5.7.

The average number of K_S^0 , $\Lambda(\bar{\Lambda})$ and charged particles produced in the decay of a b-hadron (for the mixture of b-hadrons produced at LEP) are respectively

$$\begin{aligned}
 n(B \rightarrow K_S^0 X) &= 0.290 \pm 0.011(stat) \pm 0.027(syst) \\
 n(B \rightarrow K^\pm X) &= 0.88 \pm 0.05(stat) \pm 0.18(syst) \\
 n(B \rightarrow pX) &= 0.141 \pm 0.018(stat) \pm 0.056(syst) \\
 n(B \rightarrow \Lambda X) &= 0.059 \pm 0.007(stat) \pm 0.009(syst) \\
 n(B \rightarrow Charged X) &= 5.84 \pm 0.04(stat) \pm 0.38(syst),
 \end{aligned}$$

where the errors quoted as “statistical” for the K_S^0 and Λ multiplicities include a contribution from the background estimate.

The average multiplicities of K_S^0 and K^\pm from the decays of b-hadrons are consistent with those measured at the $\Upsilon(4S)$, $(32.0 \pm 1.9)\%$ and $(80.7 \pm 4.8)\%$ respectively [37]. In particular, our result is consistent with the fact that the average K_S^0 multiplicity is less than half the average K^\pm multiplicity, against expectations based on isospin considerations. The fractions of inclusive Λ and inclusive proton production in the decay of nonstrange B mesons have been measured at the $\Upsilon(4S)$ to be $(4.0 \pm 0.5)\%$ and $(8.0 \pm 0.5)\%$ respectively [20]. The average multiplicity of Λ and p in the decays of b-hadrons at LEP is expected to be bigger because of the presence of b-baryons. From the difference of the inclusive branching fraction of the b-hadrons into Λ measured at LEP and at the $\Upsilon(4S)$, the branching fraction of any b-baryon (“ Λ_b ”) into Λ plus anything has been determined as:

$$Br(\Lambda_b \rightarrow \Lambda X) = 0.28_{-0.12}^{+0.17}.$$

Acknowledgements

We are greatly indebted to our technical collaborators and to the funding agencies for their support in building and operating the DELPHI detector, and to the members of the CERN-SL Division for the excellent performance of the LEP collider.

References

- [1] B.A. Schumm et al. (MARK II Coll.), *Phys. Rev.* **D46** (1992) 453.
- [2] R. Akers et al. (OPAL Coll.), *Zeit. Phys.* **C61** (1994) 209.
- [3] K. Abe et al. (SLD Coll.), *Phys. Rev. Lett.* **72** (1994) 3145.
- [4] T. Sjöstrand, *Comp. Phys. Comm.* **28** (1983) 229; T Sjöstrand, *PYTHIA 5.6 and JETSET 7.3*, CERN-TH.6488/92 (1992).
- [5] P. Aarnio et al. (DELPHI Coll.), *Nucl. Instr. Meth.* **A303** (1991) 233.
- [6] P. Aarnio et al. (DELPHI Coll.), *Phys. Lett.* **B240** (1990) 271.
- [7] W. Adam et al., Contributed paper n. gls0188 to the XXVII Int. Conf. on High Energy Physics, Glasgow, U.K., July 1994 (DELPHI 94-112 PHYS 429).
- [8] *DELSIM User Manual*, DELPHI 87-96 PROG-99, CERN, July 1989.
DELSIM Reference Manual, DELPHI 87-98 PROG-100, CERN, July 1989.
- [9] C. Peterson, D. Schlatter, I. Schmitt and P.M. Zerwas, *Phys. Rev.* **D27** (1983) 105.
- [10] G. Marchesini and B.R. Webber, *Nucl. Phys.* **B238** (1984) 1.
- [11] L. Lönnblad, DESY 92-046.
- [12] D. Buskulic et al. (ALEPH Coll.), *Phys. Lett.* **B313** (1993) 535.
- [13] P. Abreu et al. (DELPHI Coll.), Measurement of the $\Gamma_{b\bar{b}}/\Gamma_{had}$ Branching Ratio of the Z by Double Hemisphere Tagging, CERN-PPE/94-131, submitted to *Zeit. Phys. C*.
- [14] See for example: A.S. Schwarz, *Phys. Rep.* **238** (1994) 1 and references therein.
- [15] P. Abreu et al. (DELPHI Coll.), Production Characteristics of K^0 and Light Meson Resonances in Hadronic Decays of the Z, CERN-PPE/94-130, submitted to *Zeit. Phys. C*.
- [16] P. Baillon, *Nucl. Instr. Meth.* **A238** (1985) 341.
- [17] G.J. Alner et al. (UA5 Coll.), *Phys. Lett.* **B160** (1985) 193; A. Giovannini and L. Van Hove, *Zeit. Phys.* **C30** (1986) 391.
- [18] P. Abreu et al. (DELPHI Coll.), *Zeit. Phys.* **C50** (1991) 185.
- [19] W. Venus, *Proc. XVIIth Int. Symp. on Lepton and Photon Interactions*, Ithaca, New York, August 1993, Eds. P. Drell and D. Rubin, AIP, New York, 1994, p. 274.
- [20] Particle Data Group, *Review of Particle Properties*, *Phys. Rev.* **D50** (1994).
- [21] The LEP Coll. (ALEPH, DELPHI, L3, OPAL) and the LEP Electroweak Working Group, "Updated Parameters of the Z Resonance from Combined Preliminary Data of the LEP Experiments", CERN-PPE/93-157.
- [22] V. Gibson, to appear in *Proc. of the XXVII Int. Conf. on High Energy Physics*, Glasgow, U.K., July 1994.
- [23] Yu.L. Dokshitzer, V.A. Khoze and S.I. Troyan, 'Perturbative Quantum Chromodynamics', Ed. A. Mueller, World Scientific, Singapore, 1989; Yu.L. Dokshitzer, V.A. Khoze, A.H. Mueller and S.I. Troyan, 'Basics of Perturbative QCD', Ed. J. Trân Thanh Vân, Editions Frontières, Gif-sur-Yvette, France, 1991.
- [24] Yu.L. Dokshitzer, V.A. Khoze and S.I. Troyan, *J. Phys.* **G17** (1991) 1481; *ibid.* **17** (1991) 1602.
- [25] D. Amati and G. Veneziano, *Phys. Lett.* **B83** (1979) 87; Ya. I. Azimov, Yu.L. Dokshitzer, V.A. Khoze and S.I. Troyan, *Zeit. Phys.* **C27** (1985) 65.
- [26] B.A. Schumm, Y.L. Dokshitzer, V.A. Khoze and D.S. Koetke, *Phys. Rev. Lett.* **69** (1992) 3025.
- [27] V.A. Petrov and A.V. Kisselev, On Hadron Multiplicities in e^+e^- Events Induced by Massive Quarks, CERN-TH 7318/94.
- [28] J. Dias de Deus, Heavy Quarks and Multiplicity Distributions in e^+e^- Annihilations,

- CERN-TH 7380/94.
- [29] P.C. Rowson et al. (MARK II Coll.), *Phys. Rev. Lett.* **54** (1985) 2580; A.V. Kisselev, V.A. Petrov and O.P. Yushchenko, *Zeit. Phys.* **C41** (1988) 521.
- [30] J. Chrin, to appear in *Proc. of the XXVII Int. Conf. on High Energy Physics*, Glasgow, U.K., July 1994; A Study of The Difference in Charged Multiplicity Between Bottom and Light Quark Initiated Events, University of Valencia preprint IFIC/94-37; P. Abreu et al. (DELPHI Coll.), contributed paper n. gls0184 to the XXVII Int. Conf. on High Energy Physics, Glasgow, U.K., July 1994 (DELPHI 94-64 PHYS 385); R. Akers et al. (OPAL Coll.), *Zeit. Phys.* **C61** (1994) 209; K. Abe et al. (SLD Coll.), *Phys. Rev. Lett.* **72** (1994) 3145; B.A. Schumm et al. (MARK II Coll.), *Phys. Rev.* **D46** (1992) 453; K. Nagai et al. (TOPAZ Coll.), *Phys. Lett.* **B278** (1992) 506; W. Braunschweig et al. (TASSO Coll.), *Zeit. Phys.* **C42** (1989) 17; M. Sakuda et al. (DELCO Coll.), *Phys. Lett.* **B152** (1985) 399; H. Aihara et al. (TPC Coll.), *Phys. Lett.* **B184** (1987) 299; P.C. Rowson et al. (MARK II Coll.), *Phys. Rev. Lett.* **54** (1985) 2580.
- [31] J. Chrin, *Zeit. Phys.* **C36** (1987) 163.
- [32] R. Giles et al. (CLEO Coll.), *Phys. Rev.* **D30** (1984) 2279; H. Albrecht et al. (ARGUS Coll.), *Zeit. Phys.* **C54** (1992) 20.
- [33] A. Korytov et al. (DELPHI Coll.), DELPHI 91-16 PHYS 87 (April 1991).
- [34] P. Abreu et al. (DELPHI Coll.), *Phys. Lett.* **B318** (1993) 249.
- [35] P. Abreu et al. (DELPHI Coll.), Contributed paper n. gls0305 to the XXVII Int. Conf. on High Energy Physics, Glasgow, U.K., July 1994 (DELPHI 94-80 PHYS 397).
- [36] A. De Angelis, *J. Phys.* **G19** (1993) 1233.
- [37] A. De Angelis, Properties of the $Z \rightarrow b\bar{b}$ Events, CERN-PPE/94-174, to be published in the Proceedings of the XXIV Symposium on Multiparticle Dynamics (Vetri Sul Mare, Italy, September 1994);
 K_S^0 : P. Abreu et al. (DELPHI Coll.), CERN-PPE/94-130, submitted to *Zeit. Phys.* **C**; D. Buskulic et al. (ALEPH Coll.), CERN-PPE/94-74, submitted to *Zeit. Phys.* **C**; M. Acciari et al. (L3 Coll.), *Phys. Lett.* **B328** (1994) 223; G. Alexander et al. (OPAL Coll.), *Phys. Lett.* **B264** (1991) 467; P. Abreu et al. (DELPHI Coll.), *Phys. Lett.* **B275** (1992) 231;
 K^\pm and p : R. Akers et al. (OPAL Coll.), CERN-PPE/94-49; P. Abreu et al. (DELPHI Coll.), "Inclusive K^\pm and p Production in Z^0 Decays", to be submitted to *Phys. Lett.* **B**;
 Λ : P. Abreu et al. (DELPHI Coll.), *Phys. Lett.* **B318** (1993) 249; D. Buskulic et al. (ALEPH Coll.), CERN-PPE/94-74, submitted to *Zeit. Phys.* **C**; M. Acciari et al. (L3 Coll.), *Phys. Lett.* **B328** (1994) 223; G. Alexander et al. (OPAL Coll.), *Phys. Lett.* **B291** (1992) 503;
Charged Particles: P. Abreu et al. (DELPHI Coll.), *Zeit. Phys.* **C50** (1991) 185; G.S. Abrams et al. (MARK II Coll.), *Phys. Rev. Lett.* **64** (1990) 1334; P.D. Acton et al. (OPAL Coll.), *Zeit. Phys.* **C53** (1992) 539; B. Adeva et al. (L3 Coll.), *Phys. Lett.* **B259** (1991) 199; D. Decamp et al. (ALEPH Coll.), *Phys. Lett.* **B273** (1991) 181.

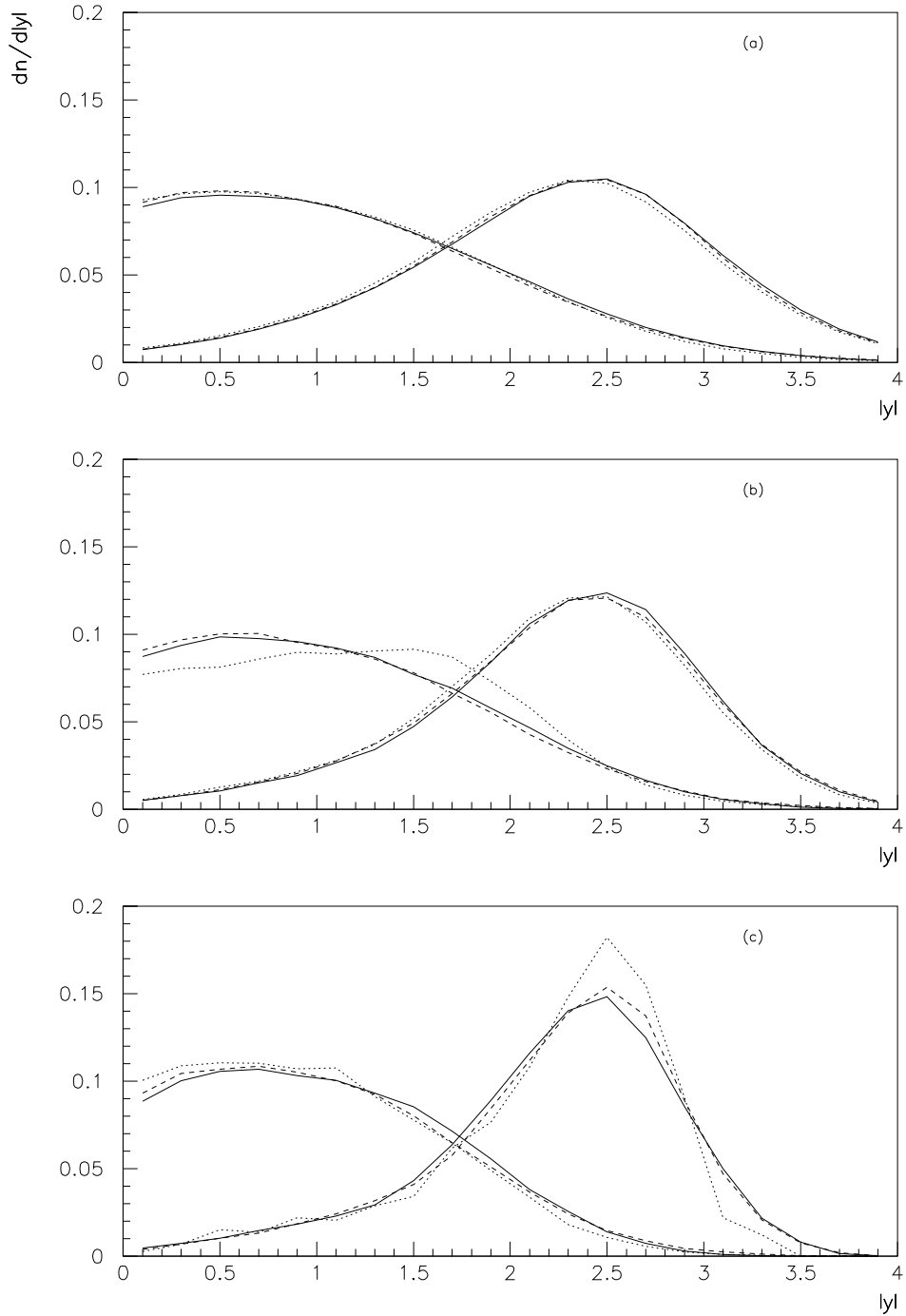


Figure 1: Rapidity distributions for (a) charged particles, (b) K^0 's, (c) Λ 's arising from fragmentation (the three curves peaking at small rapidity) and from the decay of b-hadrons (the three curves peaking at large rapidity). JETSET 7.4 PS (solid), JETSET 7.3 PS with DELPHI decay Tables (dashed) and HERWIG 5.7 (dotted). Distributions normalized to 1.

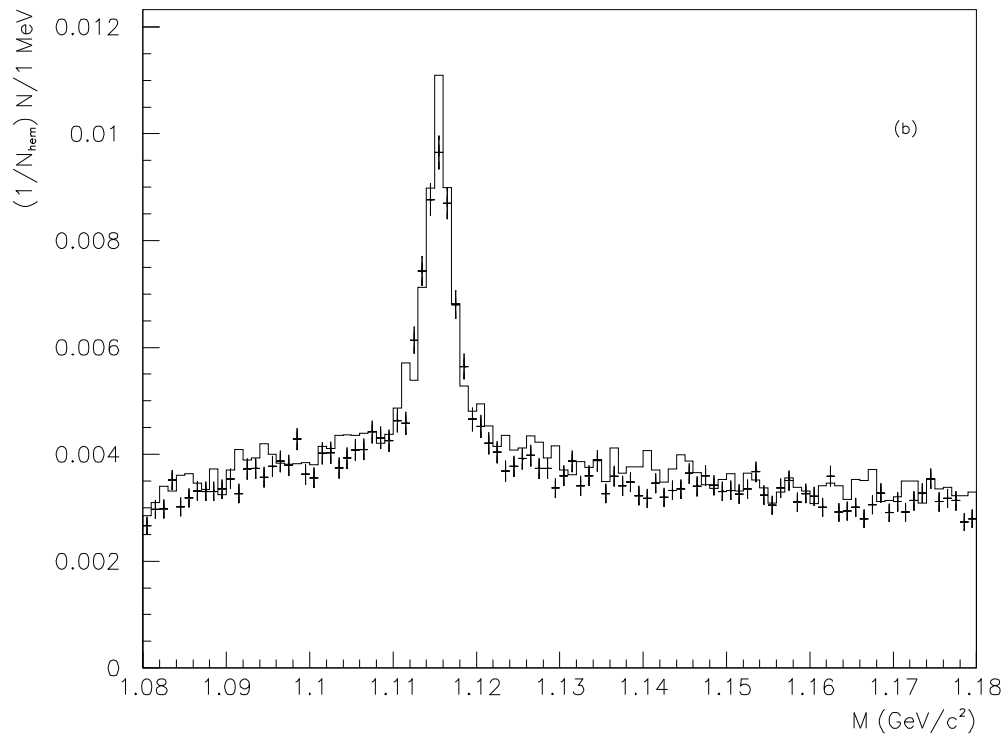
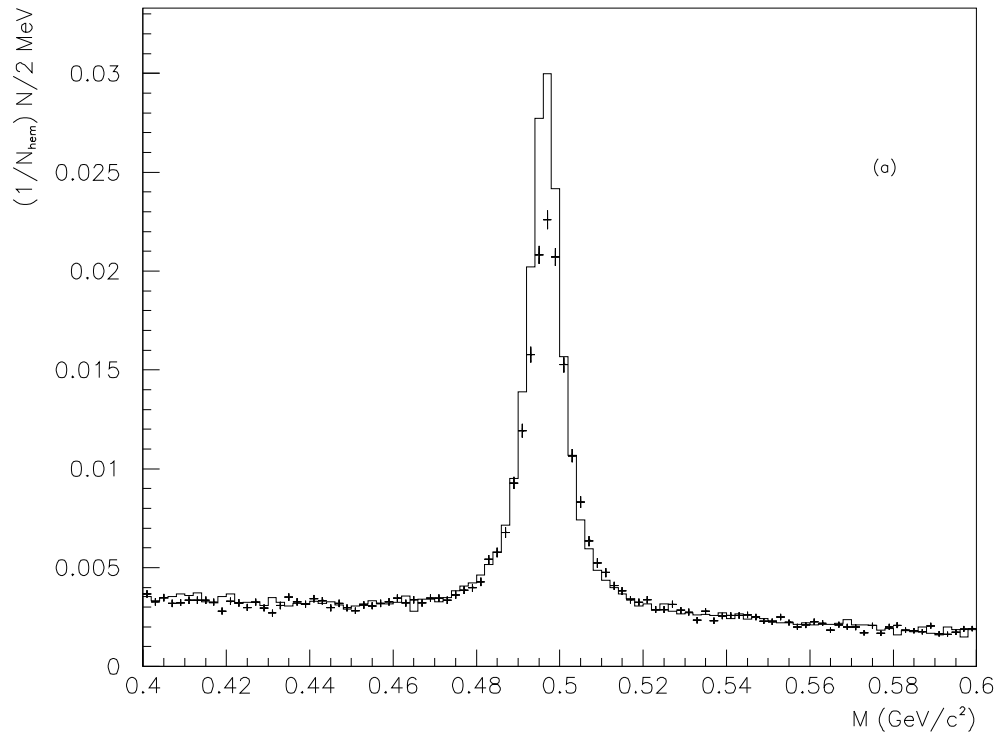


Figure 2: $\pi^+\pi^-$ invariant mass spectrum for the K_S^0 candidates (a) and $p\pi$ invariant mass spectrum for the Λ candidates in the b-tagged sample. Data (points) and simulation (line) are both normalized to the number of selected hemispheres.

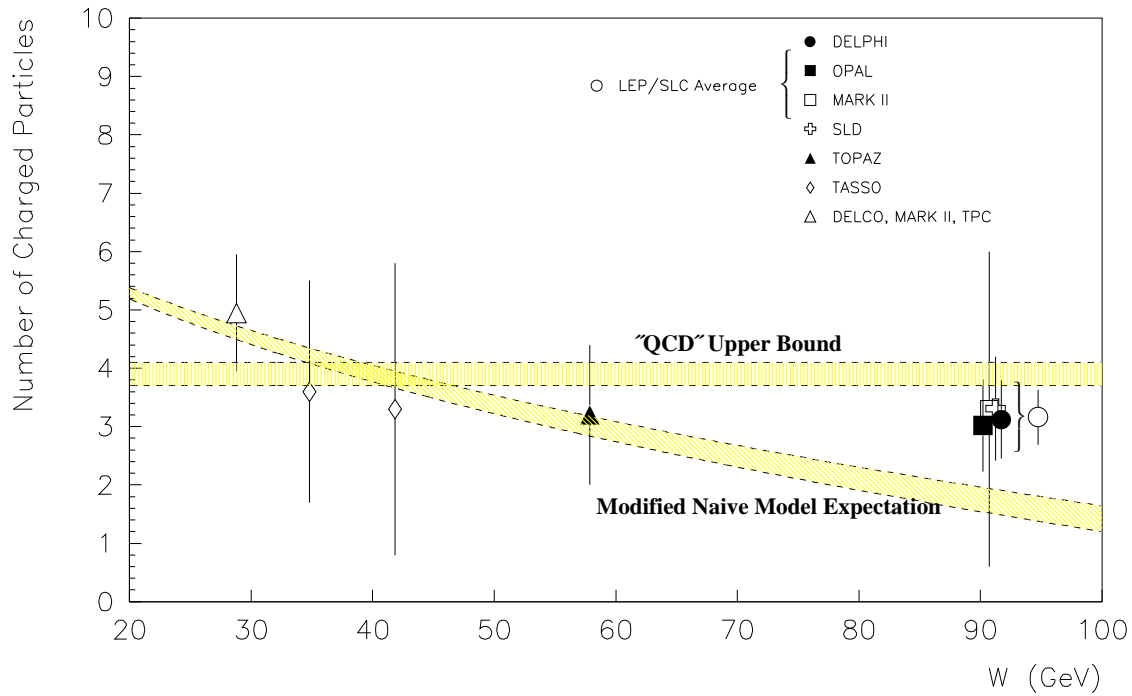


Figure 3: Experimental measurements of the charged particle multiplicity difference between b and uds events, δ_{bl} , as a function of centre-of-mass energy, W . Also shown is the QCD upper bound value of $\delta_{bl} < 3.7 - 4.1$ and the expectations from the modified naive model (the band corresponds to the range $\langle x_E \rangle_B = 0.69 - 0.73$).

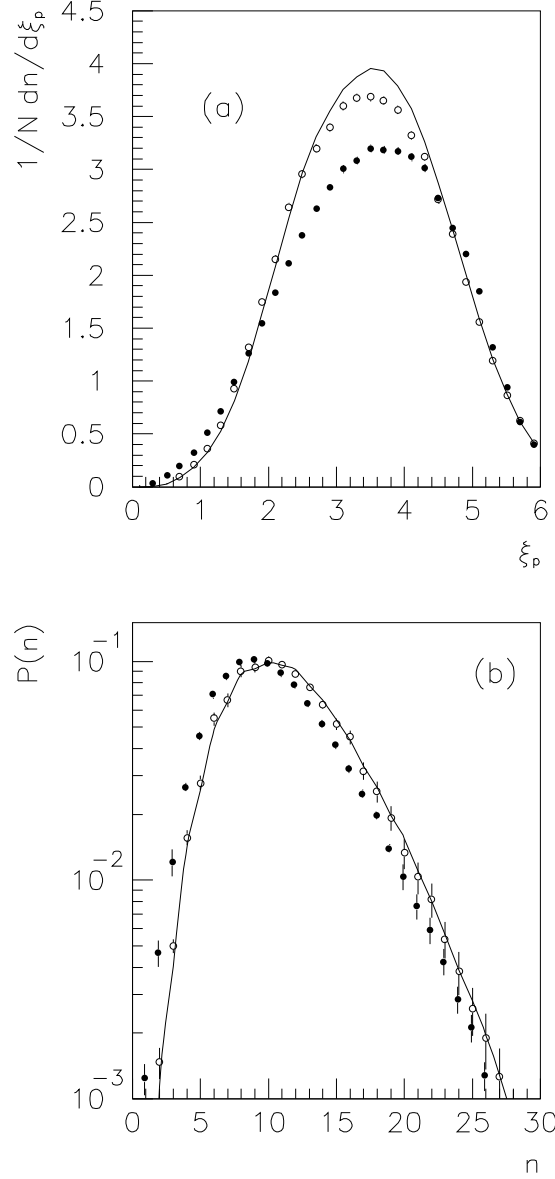


Figure 4: ξ_p (a) and multiplicity (b) distributions for charged particles in b hemispheres (open circles), normalized to the total number of hemispheres, compared to the same distributions in hadronic (untagged) events (closed circles). The predictions from JETSET 7.4 PS are drawn as solid lines.

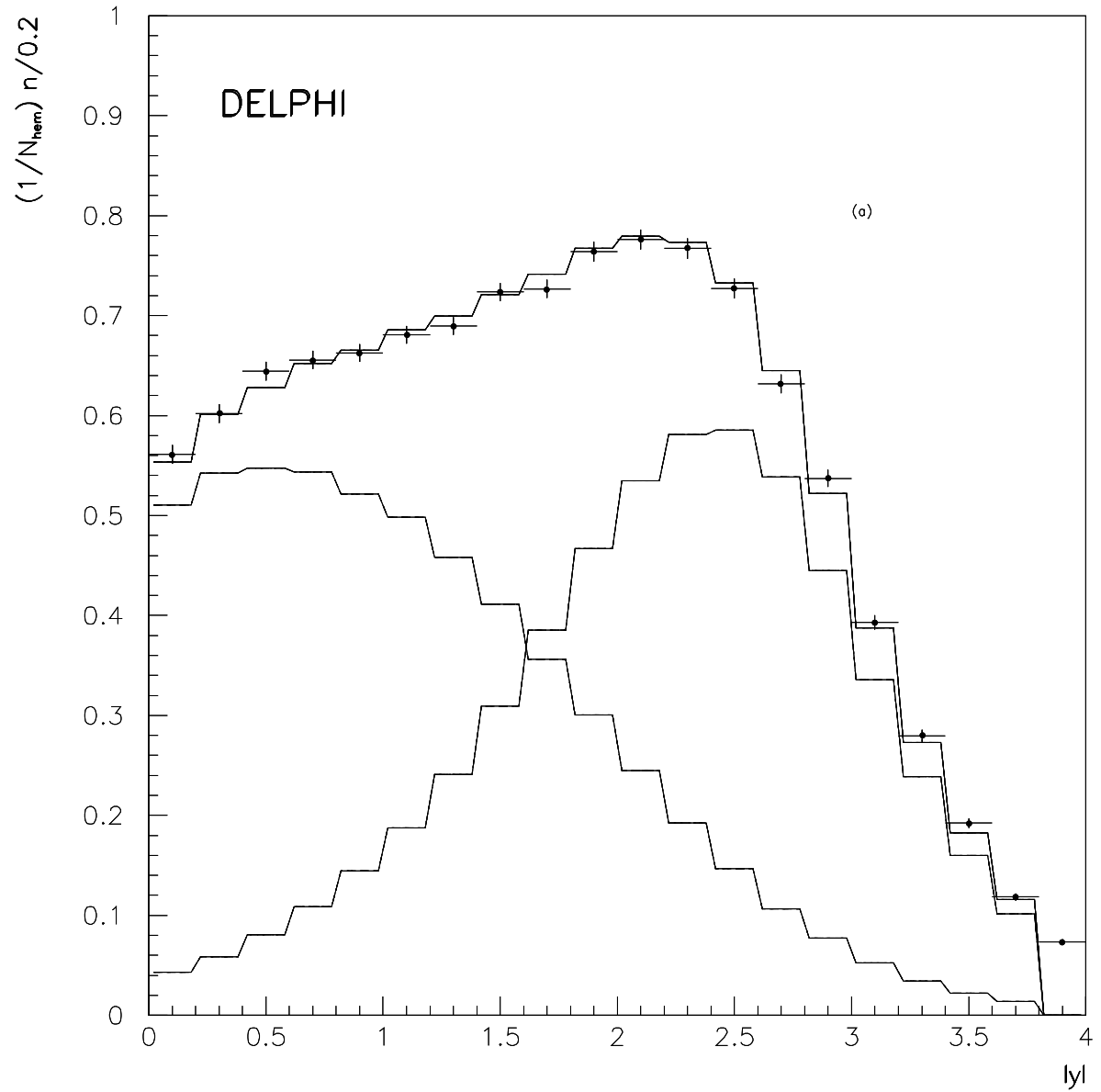


Figure 5: Rapidity distribution for (a) charged particles, (b) K_S^0 's, (c) Λ , (d) K^\pm in $b\bar{b}$ events. The two components from decay of b-hadrons and fragmentation (as in JETSET 7.3 PS) are shown; their sum is the histogram.

